Shape-Controlled Synthesis of Highly Crystalline Titania Nanocrystals

Cao-Thang Dinh,[†] Thanh-Dinh Nguyen,[†] Freddy Kleitz,[‡] and Trong-On Do[†,*]

[†]Department of Chemical Engineering and [‡]Department of Chemistry, Laval University, Quebec G1V 0A6, Canada

ABSTRACT A versatile synthetic method based on solvothermal technique has been developed for the fabrication of TiO_2 nanocrystals with different shapes such as rhombic, truncated rhombic, spherical, dog-bone, truncated and elongated rhombic, and bar. The central features of our approach are the use of water vapor as hydrolysis agent to accelerate the reaction and the use of both oleic acid and oleylamine as two distinct capping surfactants which have different binding strengths to control the growth of the TiO_2 nanoparticles. We also show that the presence of an appropriate amount of water vapor along with the desired oleic acid/oleylamine molar ratio plays a crucial role in controlling size and shape of TiO_2 nanocrystals.

KEYWORDS: nanocrystals · shape-controlled · titania · crystal growth · nanoparticles · photocatalyst

Titanium dioxide nanoparticles (TiO_2 NPs) have received a great deal of attention owing to their potential application in a wide range of fields such as photocatalysis, dye-sensitive solar cells, photochromic devices, and gas sensing.[1−7] These applications originate from the unique physical and chemical properties of TiO_2 which depend not only on the crystal phase and particle size but also on the particle shape.[8−13] For instance, Joo *et al.* demonstrated that TiO_2 nanorods exhibit superior photocatalytic inactivation of *Escherichia coli* than that of Degussa P-25.[12] Moreover, changing the shape of nanocrystals (NCs) is more flexible and provides more variable electronic states than simply changing the size of the system.[13] Controlling the shapes of TiO_2 NPs is thus of key importance in the fabrication of materials with desired properties.

There have been, over the past decades, a number of synthetic routes to the preparation of TiO_2 NPs. For example, conventional hydrolytic sol−gel process and emulsion precipitation[14−17] performed at relatively low temperature yield amorphous products with polydisperse particles, and subsequent calcination is needed to induce crystallization. Furthermore, hydrolytic reaction rates are often too high, especially with transition metal precursors, making it difficult to control the processes.[18] Because of fast hydrolytic reactions, slight changes in kinetics may lead to dramatic changes in size and shape of the final materials. Recently, a nonhydrolytic process usually conducted at elevated temperature could produce monodisperse TiO_2 NPs with high crystallinity.[19−22] The use of oxygen donors other than water in nonhydrolytic conditions results in a drastic decrease in the reaction rate, leading to a slow growth process of particles. Furthermore, for the control of TiO_2 NP morphology, in addition to the control of reaction rate, the use of surfactants which selectively adsorb on particle surfaces has also been shown to play a crucial role.[23−25] For example, Jun *et al.*[23] reported the synthesis of bullet-, diamond-, and rod-shaped TiO_2 *via* a nonhydrolytic process, which employed both lauric acid as selective surfactant and trioctylphosphine oxide as nonselective surfactant.

However, a comparatively low reaction rate of nonhydrolytic reactions compared to that of hydrolytic reactions limits severely the diversity in possible NP morphology, and as a consequence, few examples of controlled shapes of TiO_2 NPs have been reported so far. Efforts have been devoted to combine both hydrolytic and nonhydrolytic reactions in tailoring the size and shape of TiO_2 NPs by adding a certain amount of water to nonaqueous media.[26−28] For instance, Li *et al.*[26] used linoleic acid as a capping agent and water produced from the *in situ* decomposition of NH_4HCO_3 as a hydrolysis agent for the synthesis of TiO_2 NPs. Differently, Wu *et al.*[27] prepared rhombic-shaped anatase NCs by using a trace amount of water and oleylamine as hydrolysis agent and capping surfactant, respectively. Nevertheless, the

*Address correspondence to trong-on.do@gch.ulaval.ca.

Received for review August 5, 2009 and accepted September 21, 2009.

Published online October 6, 2009.
10.1021/nn900940p CCC: $40.75

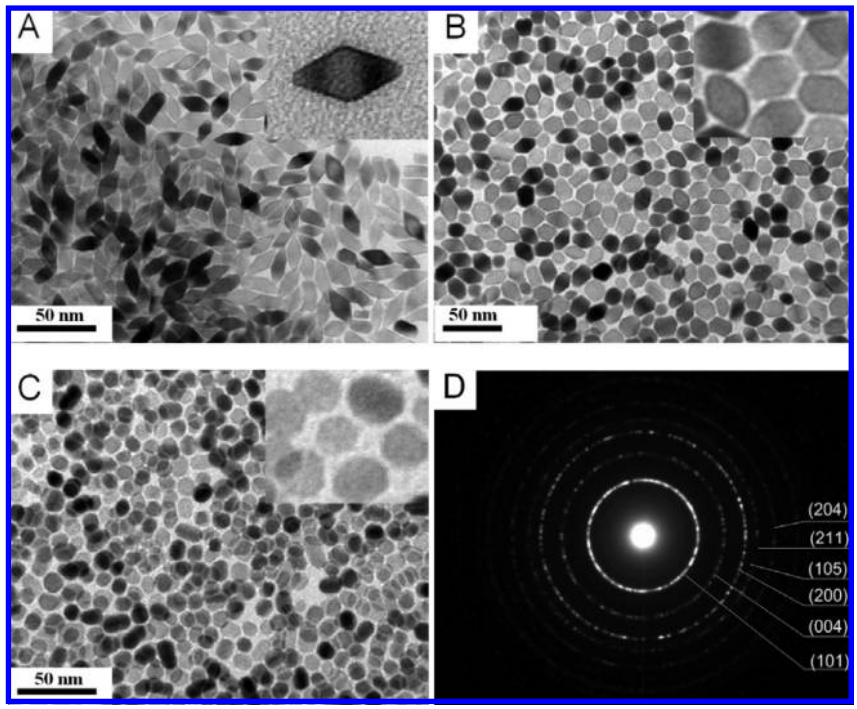

Figure 1. TEM images of (A) the rhombic shapes obtained at TB/OA/OM = 1:4:6; (B) truncated rhombic shape obtained at TB/OA/OM = 1:5:5; (C) spherical shape obtained at TB/OA/OM = 1:6:4. Insets show high-magnification images of the corresponding shapes. (D) SAED of truncated rhombic TiO_2 nanoparticles.

development of facile and reproducible syntheses of shape-controlled TiO_2 NCs with high crystallinity still remains a great challenge.

Herein, we report a new approach based on a solvothermal technique for the tailored synthesis of TiO_2 NCs with controlled shapes (*e.g.*, rhombic, truncated rhombic, spherical, dog-bone, truncated and elongated rhombic, and bar). The central features of our approach are the use of water vapor as the hydrolysis agent to accelerate the reaction and the use of both oleic acid (OA) and oleylamine (OM) as two distinct capping surfactants, which are commonly used as capping agents in shape-controlled synthesis of inorganic nanocrystals[29−31] and have different binding strengths to control the growth of the TiO_2 NCs. OA was chosen because the carboxylic acid functional groups have previously been demonstrated to tightly bind onto the TiO_2 surface and favor the formation of TiO_2 nanorods.[12,26,28] OM, on the other hand, was chosen as it was proven effective as surfactant to prepare TiO_2 nanosheets and rhombic-shaped TiO_2 nanocrystals.[27] Titanium butoxide was chosen as titanium source as it exhibits a low hydrolysis rate owing to a longer alkyl group that slows down the diffusion and polymerization processes.[32,33] Slow hydrolysis of titanium butoxide is favorable in forming TiO_2 nanocrystals with controlled morphology. We also show that the presence of an appropriate amount of water vapor along with the desired OA/OM molar ratio plays a crucial role in controlling size and shape of TiO_2 NCs.

RESULTS AND DISCUSSION

Figure 1 shows TEM images of the TiO_2 NPs synthesized by varying the OA/OM molar ratio, while leaving the molar ratio of titanium *n*-butoxide (TB) and surfactants unchanged (*i.e.*, TB/(OA + OM) = 1:10). When the OA/OM mole ratio is 4:6, rhombic-shaped TiO_2 NPs with uniform size are obtained (Figure 1A). By increasing the OA/OM molar ratio to 5:5, smaller TiO_2 NCs with truncated rhombic shape are produced (see Figure 1B and Figure S1 in Supporting Information). A further increase of this ratio up to 6:4 leads to the formation of spherical particles with an average size of 13 nm (Figure 1C). One can also point out that, in all cases studied here, no large particles were observed and the TiO_2 NPs remained monodisperse in size. The crystallinity of the synthesized samples was verified by powder X-ray diffraction (XRD). As seen in Figure S2 (Supporting Information), the XRD patterns of TiO_2 NPs with (a) rhombic, (b) truncated rhombic, and (c) spherical shapes exhibit well-defined peaks assigned to the pure anatase phase (JCPDS File No. 21-1272), indicative of the high crystallinity of these samples. The highly crystalline anatase phase is also revealed by selected area electron diffraction (SAED), as shown in Figure 1D and Figure S3 (Supporting Information). The rings can be clearly indexed to diffraction from the (101), (004), (200), (105), (211), and (204) planes of anatase. To confirm the shapes of the obtained TiO_2 NCs, we estimated the average crystallite sizes of anatase NCs by using the Scherrer formula. The average crystallite sizes of rhombic TiO_2 were estimated from the (101) and (004) diffraction peaks using the Scherrer formula to be 18 and 38 nm, respectively. Comparing with the TEM images, these two sizes correspond to the width and length of rhombic TiO_2 NCs, respectively. The thickness along the [010] direction of rhombic TiO_2 NCs is difficult to observe by TEM as these NCs have a tendency to lie in the (010) plane.[26,34] However, the thickness can be estimated using the formula $L(010) = 0.364L(211)$, where $L(010)$ is the crystallite size in the [010] direction, corresponding to the thickness of rhombic TiO_2 NCs, and $L(211)$ is the crystallite size obtained from the (211) diffraction peak.[34] From this formula, the thickness of rhombic TiO_2 NCs is found to be 9.5 nm. In the case of truncated rhombic TiO_2 NCs, the average crystallite size estimated from the (004) diffraction peak corresponding to the crystal length is about 18 nm, in good agreement with the TEM results.

It is established that the formation of TiO_2 undergoes two main steps: (i) hydrolysis of titanium precur-

sors to produce unstable hydroxyalkoxides, and (ii) subsequent condensation reactions by means of olation or oxolation to form a Ti−O−Ti network.[35] The rate of these two processes affects dramatically the shape of the final NC products. In the presence of both water and carboxylic acid, titanium alkoxide can readily react with water or acid[28,36] to form hydroxyalkoxide or carboxyalkoxide, respectively. Subsequently, the reaction between these precursors *via* a hydrolytic condensation or a nonhydrolytic condensation process produces extensive Ti−O−Ti networks. In general, in the case of titanium, the hydrolytic process is fast, while the nonhydrolytic process is relatively slow.[18] Control of the rate of these growth processes is thus essential for tuning the shape evolution of the TiO_2 particles.

In our system, a mixture of ethanol and water was used to generate water vapor which acts as the hydrolysis agent. It is assumed that TB first reacts with water vapor that is generated at elevated temperature to produce hydroxyalkoxide species. This precursor then reacts with OA to form carboxyalkoxide or with other hydroxyalkoxides through hydrolytic condensation as a function of the amount of water and OA used. Note that the formation of carboxyalkoxide is here an important step that determines the evolution of TiO_2 crystals. The existence of a carboxylic chain can effectively hinder the attack of water at the metal centers. As a result, the hydrolytic condensation is limited. For that reason, the amount of water vapor must have a great influence on the morphology of the TiO_2 particles. To help clarify this point, experiments were carried out to study the effect of water. The TB/OA/OM molar ratio was fixed at 1:6:4, and absolute ethanol or water was used instead of a mixture of ethanol/water. We observed that, when ethanol was used alone, monodisperse TiO_2 nanodots were obtained. In contrast, when only water was used, larger NPs with cubic shape and some aggregated TiO_2 NPs were found (Figure S4 in Supporting Information). These results indicated that, with a large amount of water, TB reacts vigorously with water through hydrolytic process, leading to the aggregation of the particles, whereas in the absence of water, the formation of TiO_2 NCs undergoes slow nonhydrolytic reaction, which generally produces nanodots or nanorods.[12,19,24]

It is documented that, by using surfactants possessing different functional groups with distinct binding strengths, the morphology of resulting particles may be controlled.[37−39] In the case of TiO_2, OA binds strongly to the anatase {001} faces,[23] whereas OM tends to adhere on the {101} ones.[12] The selective bindings of these surfactant molecules to different facets of TiO_2 restrict the growth in corresponding direction. In the present system, OA and OM were used not only as capping agents but also as an acid−base pair catalyst, which also contribute to increase the condensation rate without affecting the hydrolysis rate.[17] Moreover, as mentioned above, OA can react with TB or hydroxyalkoxide

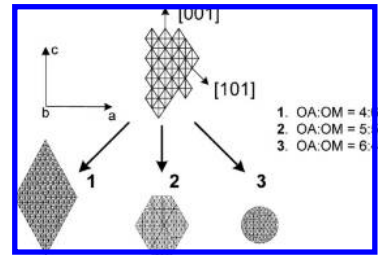

Scheme 1. Schematic representation showing the shape evolution of TiO_2 NCs as a function of the OA/OM ratio.

to generate carboxyalkoxide species which slow down the hydrolytic condensation process. OM, on other aspect, can promote the nonhydrolytic condensation process by aminolysis reaction with titanium carboxylalkoxide.[24] It is therefore expected that, by modulating the OA/OM molar ratio, the shape of TiO_2 NCs may be controlled. A series of control experiments were performed with 11 different OA/OM ratios, while keeping the amount of TB and the total surfactant amount constant to elucidate the effect of OA/OM molar ratios to the shape of TiO_2 NPs. It is found that, when the OA/OM ratio is less than 4:6, only rhombic-shaped TiO_2 NPs are formed (Figure S5, Supporting Information). The shape evolution in the range from 4:6 to 5:5 and 6:4 of the OA/OM ratio is further illustrated in Figure 1A−C. When this ratio is higher than 6:4, the NC size decreases markedly and nanodots of TiO_2 are obtained (Figure S6, Supporting Information). Moreover, two additional experiments were also performed using only OA or OM. In the absence of OA, only the rhombic shape was observed, whereas a mixture of spherical particles and nanodots is produced in the absence of OM (Figure S7, Supporting Information). These results confirm the cooperative effect of a combination of OA and OM on the resulting particle shapes.

The shape of TiO_2 NCs is determined by the growth rate ratio between [001] and [101] directions.[23,40,41] In the absence of OA or at low OA/OM ratio, hydrolytic reactions are predominant in the system, and the formation of NPs is thus a fast process. Due to high surface energy of the {001} faces,[42] growth along [001] is occurring progressively, leading to the depletion of the {001} faces. In contrast, the low surface energy of {101} faces[42] and the adhesion of OM to these faces hinder the growth along the [101] direction. As a result, rhombic-shaped TiO_2 NPs are obtained (Scheme 1). A similar observation was also reported by Wu *et al.*[27] using OM as a capping agent. Increasing the OA/OM ratio slows down the rate of the reaction. The presence of a relatively large amount of OA limits the growth along [001] as OA binds selectively to the {001} faces. Consequently, the surface area of the {001} surfaces is preserved. Crystals grow on both {001} and {101} faces, leading to the truncated rhombic or spherical NPs, as shown in Figure 1B,C. However, when a large excess of OA is used (OA/OM ratio >6:4), the growth process undergoes

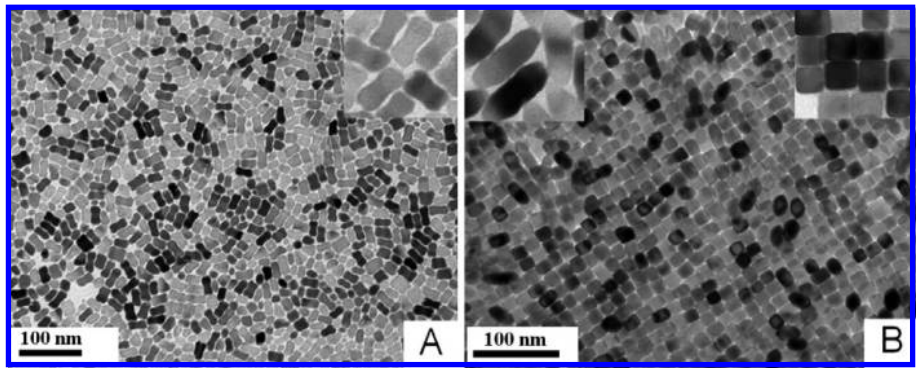

Figure 2. TEM images of (A) dog-bone-shaped TiO_2 obtained at TB/OA/OM = 2:6:4; (B) truncated and elongated rhombic TiO_2 obtained at TB/OA/OLA = 2:5:5. Insets are high-magnification images of the corresponding shapes (left, longitudinal view; right, cross view on panel B).

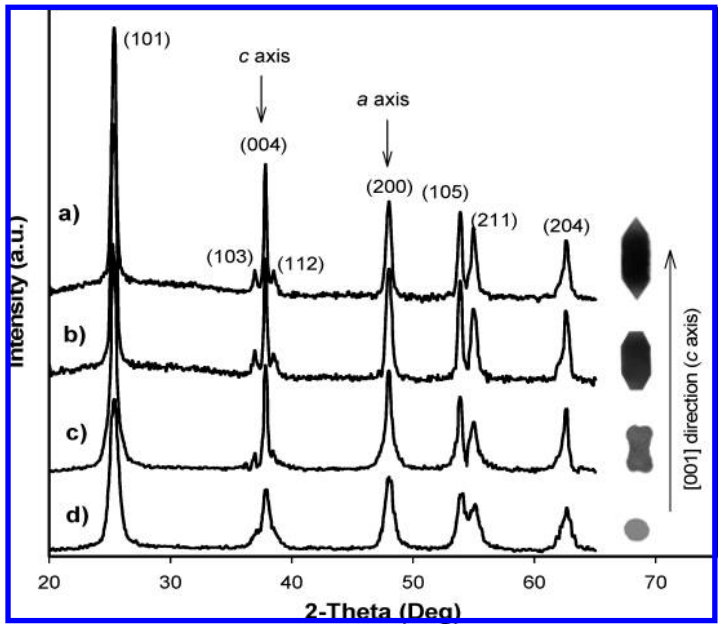

Figure 3. XRD patterns of (a) elongated rhombic-shaped TiO_2, (b) truncated and elongated rhombic-shaped TiO_2, (c) dog-bone-shaped TiO_2, and (d) spherical-shaped TiO_2. The XRD pattern of spherical-shaped TiO_2 is shown again for comparison.

nonhydrolytic condensation rather than a hydrolytic one. Since OA can be adsorbed on almost all of the surface of TiO_2, the crystals grow mainly on high surface energy faces (*i.e.*, {001} faces), leading to the formation of nanodots and nanorods.

Previous studies demonstrated that varying the amount of metal precursor also plays an important role in the size and shape evolution of NPs.[43,44] We have thus doubled the amount of TB and kept other parameters unchanged, which corresponds to the TB/OA/OM molar ratios of 2:6:4, 2:5:5, and 2:4:6 instead of 1:6:4, 1:5:5, and 1:4:6 (see Scheme S1, Supporting Information). It was found that, when a 2:6:4 ratio was applied instead of 1:6:4, the shape of TiO_2 evolved from spherical (Figure 1C) to uniform dog-bone-like particles (Figure 2A and Figure S8A in Supporting Information). This resulting shape of TiO_2 NCs is, to our knowledge, the first time found for TiO_2 NCs. For a ratio of 2:5:5 compared to 1:5:5, a change in the morphology from truncated rhombic (Figure 1B) to elongated and truncated rhombic particles was observed. The NPs tended to assemble and lay on the (001) plane (Figure 2B and Figure S8B in Supporting Information). With the 2:4:6 ratio, the formation of elongated rhombic particles was observed (Figure S9, Supporting Information) compared to the rhombic shape obtained with the 1:4:6 ratio.

The powder X-ray diffraction patterns (Figure 3) of these samples indicated their single anatase phase. In addition, the (004) diffraction peaks of these three samples appear stronger and sharper, compared to that of spherical TiO_2, suggesting the evolution along the [001] direction of TiO_2 NPs.[24] The elongation of resulting TiO_2 NCs with increasing the amount of TB may arise from anisotropic crystal growth at high monomer concentration.[44,45]

To elucidate the mechanism of formation of the elongated titania particles, we have fixed the OA/OM ratio at 6:4 and gradually increased the amount of TB. Different TB/total surfactant ratios were selected (*i.e.*, TB/total surfactant = 1.3:10, 1.6:10, 2:10, and 4:10). It is found that, with increasing the ratio from 1.3:10 to 1.6:10, the shape of TiO_2 NCs changed from elongated sphere to dumbbell, as viewed in Figure 4A,B. When the ratio was 2:10, uniform dog-bone-shaped TiO_2 was obtained (Figure 2A). However, when this ratio was further increased to 4:10, the shape of the resulting NCs remained unchanged, but larger and less uniform particles were obtained (Figure S10, Supporting Information). It is worth mentioning that, owing to the polar environment, the surfactant-capped NCs spontaneously precipitated at the bottom of the Teflon cup as they reached critical size and shape in this kinetically driven regime.

It has been demonstrated before that the reaction temperature has a great influence on tuning the morphology of different kinds of NCs.[46,47] We have fixed the TB/OA/OM ratio at 1:6:4 and conducted experiments with the temperature selected in the range of 100−180 °C to investigate the effect of the reaction temperature on the shape of TiO_2 NCs. The results revealed that no TiO_2 particles were observed at 100 °C. When the temperature was increased to 120 °C, small TiO_2 nanodots were obtained, as illustrated in Figure S11 (Supporting Information). Increasing the temperature to 140 °C led to the formation of uniform nanobars of TiO_2 with a size of *ca.* 11 × 20 nm, as observed in Figure 5A and Figure S12 (Supporting Information). To the best of our knowledge, although various shapes of TiO_2 NCs have

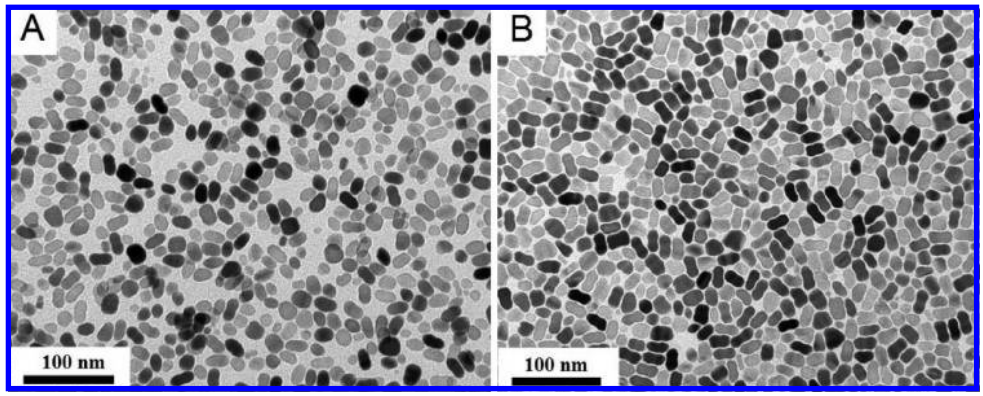

Figure 4. TEM images of (A) elongated spherical TiO_2 obtained at TB/OA/OM = 1.3:6:4; (B) dumbbell TiO_2 obtained at TB/OA/OM = 1.6:6:4.

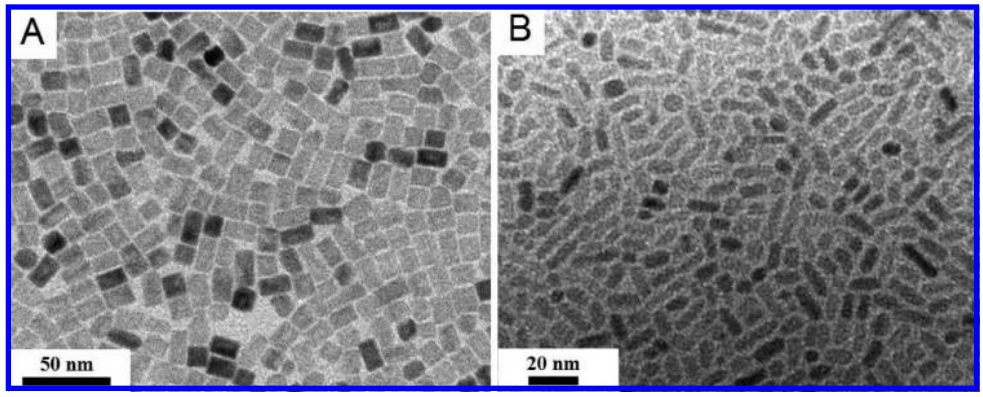

Figure 5. TEM images of (A) TiO_2 nanobars obtained with TB/OA/OM = 1:6:4 at 140 °C; (B) TiO_2 nanodots obtained with TB/OA/OLA = 1:7:3 at 140 °C.

been synthesized, the synthesis of such monodisperse TiO_2 nanobars has not been reported yet. When the reaction was performed at 160 °C, a mixture of spherical particles and nanodots of TiO_2 was observed (Figure S13, Supporting Information). However, further increasing the temperature to 180 °C yielded uniform TiO_2 NCs with spherical shape, as shown in Figure 1C. When the reaction temperature was increased, the shape of TiO_2 NCs evolved from an anisotropic form to an isotropic one (*i.e.*, from nanodots to spherical particles). This can be ascribed to the balance between the kinetic and thermodynamic growth regimes.[47] In the kinetic regime, the crystals grow rapidly on the faces with high surface energy, leading to TiO_2 nanodots. However, when the growth temperature is increased to a value that provides sufficient thermal energy, the shapes of TiO_2 NCs change to more thermodynamically stable spherical shapes through the intraparticle ripening and interparticle Ostwald ripening processes.

We have thus demonstrated above that the application of relatively high OA/OM molar ratio (*i.e.*, OA/OM ratio >6:4) leads to the formation of nanodots and nanorods, that nanodots could be obtained at low temperature, and that variation of OA/OM ratio changed the shape of TiO_2 NCs. On the basis of these results, additional experiments were performed with applying different TB/OA/OM molar ratios (*i.e.*, TB/OA/OM = 1:7:3 and 1:8:2) at relatively low temperature (*i.e.*, 140 °C) to obtain TiO_2 nanodots with different aspect ratios. As expected, the diameter of the resulting nanodots decreases dramatically while the nanodot length decreases only slightly with increasing OA/OM ratio (see Figure 5A,B and Figure S14, Supporting Information). The nanodot diameter decreases from 11 to 6 nm and to 3 nm with increasing OA/OM ratio from 6:4 to 7:3 and to 8:2, respectively, while the nanodot length is essentially intact. This result can be interpreted by the fact

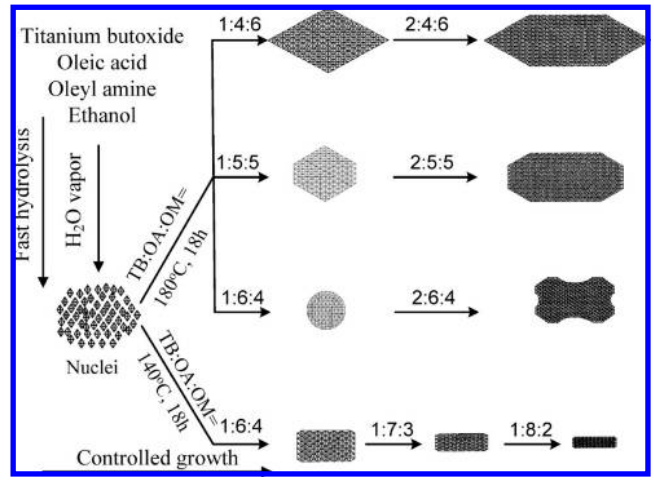

Scheme 2. Schematic illustration of the overall formation and shape evolution of TiO_2 NCs.

that, when a large amount of OA is employed, the adsorption of OA on {001} faces is saturated. As a high OA concentration in the synthesis solution, OA also adsorbs on the {101} faces. This could eventually inhibit the growth in the [101] direction. As a result, the diameter of nanodots decreases substantially with increasing the OA concentration. The formation mechanism and shape evolution of TiO_2 NCs can be schematically illustrated in Scheme 2.

CONCLUSION

In conclusion, we have demonstrated the synthesis of TiO_2 nanocrystals with various shapes, such as rhombic, truncated rhombic, spherical, dog-bone, truncated and elongated rhombic, bar, and dots, by using a simple solvothermal route employing both OA and OM as capping agents in the presence of water vapor. In this system, a simple variation of the OA/OM molar ratio or the amount of TB or reaction temperature enables a fine control of the growth rate of TiO_2 NCs and, consequently, a control of the shape of these particles. Such nanocrystals with controlled shape and size will be valuable for further investigation of shape-dependent properties of TiO_2. Future work is in progress to gain further insight into mechanistic aspects as well as the study of photocatalytic activities of these materials. Moreover, this new approach may be extended to the shape-controlled synthesis of other transition metal oxides and their mixed oxides.

EXPERIMENTAL DETAILS

Chemicals: All chemicals were used as received; titanium(IV) butoxide (TB, 97%), oleic acid (OA, 90%), and oleylamine (OM, 70%) were purchased form Aldrich. Absolute ethanol and toluene solvents were of analytical grade and were also purchased from Aldrich.

Synthesis of TiO_2 NCs: The synthesis of TiO_2 NCs with various shapes was accomplished using a solvothermal method. Typically, TB (5−10 mmol) was added to a mixture of *X* mmol OA, *Y* mmol OM, and 100 mmol absolute ethanol ($X + Y = 50$). *X* and *Y* were varied to gain different OA/OM ratios. For example, to synthesize TiO_2 with truncated rhombic shape, 5 mmol of TB was added to a mixture of 25 mmol OA, 25 mmol OM, and 100 mmol absolute ethanol. The obtained mixture in a 40 mL Teflon cup was stirred for 10 min before being transferred into a 100 mL Teflon-lined stainless steel autoclave containing 20 mL of a mixture of ethanol and water (96% ethanol, v/v; see Scheme S1, Supporting Information). The concentration of ethanol was used at the azeotropic point so that the amount of water vapor did not change much during the crystallization process. The system was then heated at 180 °C for 18 h. The obtained white precipitates were washed several times with ethanol and then dried at room temperature. The as-synthesized TiO_2 NP products were dispersed in nonpolar solvent, such as toluene. To investigate the effect of water on size and shape of resulting TiO_2 NPs, two experiments with pure absolute ethanol and with pure water were also carried out.

Characterization: Transmission electron microscope (TEM) images and selected area electron diffraction (SAED) of TiO_2 NPs were obtained on a JEOL JEM 1230 operated at 120 kV. Samples were prepared by placing a drop of a dilute toluene dispersion of nanocrystals onto a 200 mesh carbon-coated copper grid and evaporated immediately at ambient temperature. The X-ray diffraction patterns of the samples were obtained on a Bruker SMART APEXII X-ray diffractometer operated at 1200 W power (40 kV, 30 mA) and equipped with a Cu Kα radiation source (λ = 1.5418 Å).

Acknowledgment. This work was supported by the Natural Sciences and Engineering Research Council of Canada (NSERC) through a strategic project. F.K. thanks the Canadian Government for the Canada Research Chair on Functional nanostructured materials.

Supporting Information Available: Schematic illustration of the synthesis of TiO_2 NCs with different sizes and shapes. Additional TEM images, XRD, and SAED images of TiO_2 NCs. This material is available free of charge *via* the Internet at http://pubs.acs.org.

REFERENCES AND NOTES

1. Fujishima, A.; Honda, K. Electrochemical Photolysis of Water at a Semiconductor Electrode. *Nature* **1972**, *238*, 37–38.
2. Grätzel, M. Photoelectrochemical Cells. *Nature* **2001**, *414*, 338–344.
3. Barbe, C. J.; Arendse, F.; Comte, P.; Jirousek, M.; Lenzmann, F.; Shklover, V.; Grätzel, M. Nanocrystalline Titanium Oxide Electrodes for Photovoltaic Applications. *J. Am. Ceram. Soc.* **1997**, *80*, 3157–3171.
4. O'Regan, B.; Grätzel, M. A Low-Cost, High-Efficiency Solar Cell Based on Dye-Sensitized Colloidal TiO_2 Films. *Nature* **1991**, *353*, 737–740.
5. Chen, X.; Mao, S. S. Titanium Dioxide Nanomaterials: Synthesis, Properties, Modifications, and Applications. *Chem. Rev.* **2007**, *107*, 2891–2959.
6. Rozhkova, E. A.; Ulasov, I.; Lai, B.; Dimitrijevic, N. M.; Lesniak, M. S.; Rajh, T. A High-Performance Nanobio Photocatalyst for Targeted Brain Cancer Therapy. *Nano Lett.* **2009**, *9*, 3337–3342.
7. Wang, D.; Choi, D.; Li, J.; Yang, Z.; Nie, Z.; Kou, R.; Hu, D.; Wang, C.; Saraf, L. V.; Zhang, J.; Aksay, I. A.; Liu, J. Self-Assembled TiO_2-Graphene Hybrid Nanostructures for Enhanced Li-Ion Insertion. *ACS Nano* **2009**, *3*, 907–914.
8. Yang, H. G.; Sun, C. H.; Qiao, S. Z.; Zou, J.; Liu, G.; Smith, S. C.; Cheng, H. M.; Lu, G. Q. Anatase TiO_2 Single Crystals with a Large Percentage of Reactive Facets. *Nature* **2008**, *453*, 638–641.
9. Yang, H.; Liu, G.; Qiao, S.; Sun, C.; Jin, Y.; Smith, S. C.; Zou, J.; Cheng, H. M.; Lu, G. Q. Solvothermal Synthesis and Photoreactivity of Anatase TiO_2 Nanosheets with Dominant {001} Facets. *J. Am. Chem. Soc.* **2009**, *131*, 4078–4083.
10. Han, X.; Kuang, Q.; Jin, M.; Xie, Z.; Zheng, L. Synthesis of Titania Nanosheets with a High Percentage of Exposed (001) Facets and Related Photocatalytic Properties. *J. Am. Chem. Soc.* **2009**, *131*, 3152–3153.
11. Dai, Y.; Cobley, C. M.; Zeng, J.; Sun, Y.; Xia, Y. Synthesis of Anatase TiO_2 Nanocrystals with Exposed {001} Facets. *Nano Lett.* **2009**, *9*, 2455–2459.
12. Joo, J.; Kwon, S. G.; Yu, T.; Cho, M.; Lee, J.; Yoon, J.; Hyeon, T. Large-Scale Synthesis of TiO_2 Nanorods *via* Nonhydrolytic Sol−Gel Ester Elimination Reaction and Their Application to Photocatalytic Inactivation of *E. coli*. *J. Phys. Chem. B* **2005**, *109*, 15297–15302.
13. Li, J.; Wang, L. W. Shape Effects on Electronic States of Nanocrystals. *Nano Lett.* **2003**, *3*, 1357–1363.
14. Sugimoto, T.; Zhou, X.; Muramatsu, A. Synthesis of Uniform Anatase TiO_2 Nanoparticles by Gel−Sol Method: 4. Shape Control. *J. Colloid Interface Sci.* **2003**, *259*, 53–61.
15. Kanie, K.; Sugimoto, T. Shape Control of Anatase TiO_2 Nanoparticles by Amino Acids in a Gel−Sol System. *Chem. Commun.* **2004**, 1584–1585.

16. Lin, J.; Lin, Y.; Liu, P.; Meziani, M. J.; Allard, L. F.; Sun, Y. P. Hot-Fluid Annealing for Crystalline Titanium Dioxide Nanoparticles in Stable Suspension. *J. Am. Chem. Soc.* **2002**, *124*, 11514–11518.
17. Murakami, Y.; Matsumoto, T.; Takasu, Y. Salt Catalysts Containing Basic Anions and Acidic Cations for the Sol−Gel Process of Titanium Alkoxide: Controlling the Kinetics and Dimensionality of the Resultant Titanium Oxide. *J. Phys. Chem. B* **1999**, *103*, 1836–1840.
18. Mutin, P. H.; Vioux, A. Nonhydrolytic Processing of Oxide-Based Materials: Simple Routes to Control Homogeneity, Morphology, and Nanostructure. *Chem. Mater.* **2009**, *21*, 582–596.
19. Hay, J. N.; Raval, H. M. Synthesis of Organic−Inorganic Hybrids *via* the Non-hydrolytic Sol−Gel Process. *Chem. Mater.* **2001**, *13*, 3396–3403.
20. Arnal, P.; Corriu, R. J. P.; Leclercq, D.; Mutin, P. H.; Vioux, A. A Solution Chemistry Study of Nonhydrolytic Sol−Gel Routes to Titania. *Chem. Mater.* **1997**, *9*, 694–698.
21. Niederberger, M.; Bartl, M. H.; Stucky, G. D. Benzyl Alcohol and Transition Metal Chlorides as a Versatile Reaction System for the Nonaqueous and Low-Temperature Synthesis of Crystalline Nano-Objects with Controlled Dimensionality. *J. Am. Chem. Soc.* **2002**, *124*, 13642–13643.
22. Trentler, T. J.; Denler, T. E.; Bertone, J. F.; Agrwal, A.; Colvin, V. L. Synthesis of TiO_2 Nanocrystals by Nonhydrolytic Solution-Based Reactions. *J. Am. Chem. Soc.* **1999**, *121*, 1613–1614.
23. Jun, Y. W.; Casula, M. F.; Sim, J.-H.; Kim, S. Y.; Cheon, J.; Alivisatos, A. P. Surfactant-Assisted Elimination of a High Energy Facet as a Means of Controlling the Shapes of TiO_2 Nanocrystals. *J. Am. Chem. Soc.* **2003**, *125*, 15981–15985.
24. Zhang, Z.; Zhong, X.; Liu, S.; Li, D.; Han, M. Aminolysis Route to Monodisperse Titania Nanorods with Tunable Aspect Ratio. *Angew. Chem., Int. Ed.* **2005**, *44*, 3466–3470.
25. Buonsanti, R.; Grillo, V.; Carlino, E.; Giannini, C.; Kipp, T.; Cingolani, R.; Cozzoli, D. Nonhydrolytic Synthesis of High-Quality Anisotropically Shaped Brookite TiO_2 Nanocrystals. *J. Am. Chem. Soc.* **2008**, *130*, 11223–11233.
26. Li, X. L.; Peng, Q.; Yi, J. X.; Wang, X.; Li, Y. D. Near Monodisperse TiO_2 Nanoparticles and Nanorods. *Chem.—Eur. J.* **2006**, *12*, 2383–2391.
27. Wu, B. H.; Guo, G. Y.; Zheng, N. F.; Xie, Z. X.; Stucky, G. D. Nonaqueous Production of Nanostructured Anatase with High-Energy Facets. *J. Am. Chem. Soc.* **2008**, *130*, 17563–17567.
28. Cozzoli, P. D.; Kornowski, A.; Weller, H. Low-Temperature Synthesis of Soluble and Processable Organic-Capped Anatase TiO_2 Nanorods. *J. Am. Chem. Soc.* **2003**, *125*, 14539–14548.
29. Yin, Y.; Alivisatos, A. P. Colloidal Nanocrystal Synthesis and the Organic−Inorganic Interface. *Nature* **2005**, *437*, 664–670.
30. Kwon, S. G.; Hyeon, T. Colloidal Chemical Synthesis and Formation Kinetics of Uniformly Sized Nanocrystals of Metals, Oxides, and Chalcogenides. *Acc. Chem. Res.* **2008**, *41*, 1696–1709.
31. Wang, X.; Peng, Q.; Li, Y. Interface-Mediated Growth of Monodispersed Nanostructures. *Acc. Chem. Res.* **2007**, *40*, 635–643.
32. Golubko, N. V.; Yanovskaya, M. I.; Romm, I. P.; Ozerin, A. N. Hydrolysis of Titanium Alkoxides: Thermochemical, Electron Microscopy, SAXS Studies. *J. Sol−Gel Sci. Technol.* **2001**, *20*, 245–262.
33. Yoldas, B. E. Hydrolysis of Titanium Alkoxide and Effects of Hydrolytic Polycondensation Parameters. *J. Mater. Sci.* **1986**, *21*, 1087–1092.
34. Wen, P. H.; Itoh, H.; Tang, W. P.; Feng, Q. Single Nanocrystals of Anatase-Type TiO_2 Prepared from Layered Titanate Nanosheets: Formation Mechanism and Characterization of Surface Properties. *Langmuir* **2007**, *23*, 11782–11790.
35. Livage, J.; Henry, M.; Sanchez, C. Sol−Gel Chemistry of Transition Metal Oxides. *Prog. Solid State Chem.* **1988**, *18*, 259–341.
36. Doeuff, S.; Dromzee, Y.; Taulelle, F.; Sanchez, C. Synthesis and Solid- and Liquid-State Characterization of a Hexameric Cluster of Titanium(IV): $Ti_6(\mu^2\text{-}O)2(\mu^3\text{-}O)_2\text{-}(\mu^2\text{-}OC_4H_9)_2(OC_4H_9)_6(OCOCH_3)_8$. *Inorg. Chem.* **1989**, *28*, 4439–4445.
37. Ramirez, E.; Jansat, S.; Philippot, K.; Lecante, P.; Gomez, M.; Masdeu-Bulto, A. M.; Chaudret, B. Influence of Organic Ligands on the Stabilization of Palladium Nanoparticles. *J. Organomet. Chem.* **2004**, *689*, 4601–4610.
38. Mai, H. X.; Zhang, Y. W.; Si, R.; Yan, Z. G.; Sun, L. D.; You, L. P.; Yan, C. H. High-Quality Sodium Rare-Earth Fluoride Nanocrystals: Controlled Synthesis and Optical Properties. *J. Am. Chem. Soc.* **2006**, *128*, 6426–6436.
39. Watt, J.; Young, N.; Haigh, S.; Kirkland, A.; Tilley, R. D. Synthesis and Structural Characterization of Branched Palladium Nanostructures. *Adv. Mater.* **2009**, *21*, 2288–2293.
40. Penn, R. L.; Banfield, J. F. Morphology Development and Crystal Growth in Nanocrystalline Aggregates under Hydrothermal Conditions: Insights from Titania. *Geochim. Cosmochim. Acta* **1999**, *63*, 1549–1557.
41. Chemseddine, A.; Moritz, T. Nanostructuring Titania: Control over Nanocrystal Structure, Size, Shape, and Organization. *Eur. J. Inorg. Chem.* **1999**, 235–245.
42. Donnay, J. D.; Harker, D. A New Law of Crystal Morphology Extending the Law of Bravais. *Am. Mineral.* **1937**, *22*, 446.
43. Nguyen, T. D.; Do, T. O. General Two-Phase Routes to Synthesize Colloidal Metal Oxide Nanocrystals: Simple Synthesis and Ordered Self-Assembly Structures. *J. Phys. Chem. C* **2009**, *113*, 11204–11214.
44. Peng, Z. A.; Peng, X. Mechanisms of the Shape Evolution of CdSe Nanocrystals. *J. Am. Chem. Soc.* **2001**, *123*, 1389–1395.
45. Lee, S.-M.; Cho, S.-N.; Cheon, J. Anisotropic Shape Control of Colloidal Inorganic Nanocrystals. *Adv. Mater.* **2003**, *15*, 441–444.
46. Nguyen, T. D.; Mrabet, D.; Do, T. O. Controlled Self-Assembly of Sm_2O_3 Nanoparticles into Nanorods: Simple and Large Scale Synthesis Using Bulk Sm_2O_3 Powders. *J. Phys. Chem. C* **2008**, *112*, 15226–15235.
47. Jun, Y.-W.; Jung, Y.-Y.; Cheon, J. Architectural Control of Magnetic Semiconductor Nanocrystals. *J. Am. Chem. Soc.* **2001**, *124*, 615–619.

Supporting Information

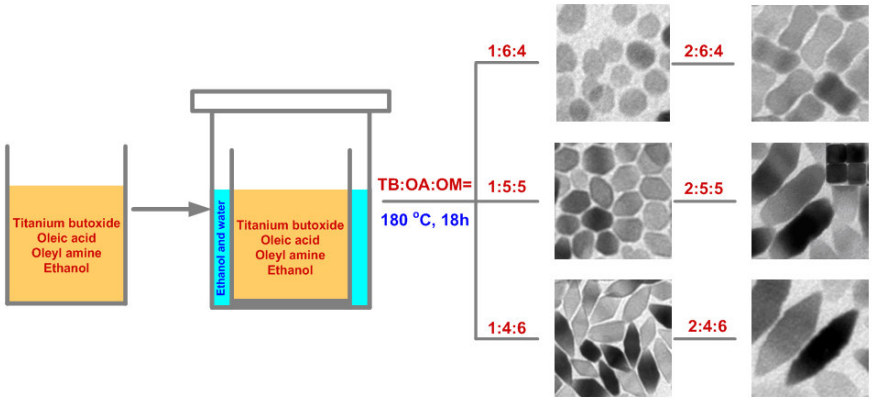

Scheme S1. Schematic illustration of the synthesis of TiO_2 nanocrystals with different sizes and shapes.

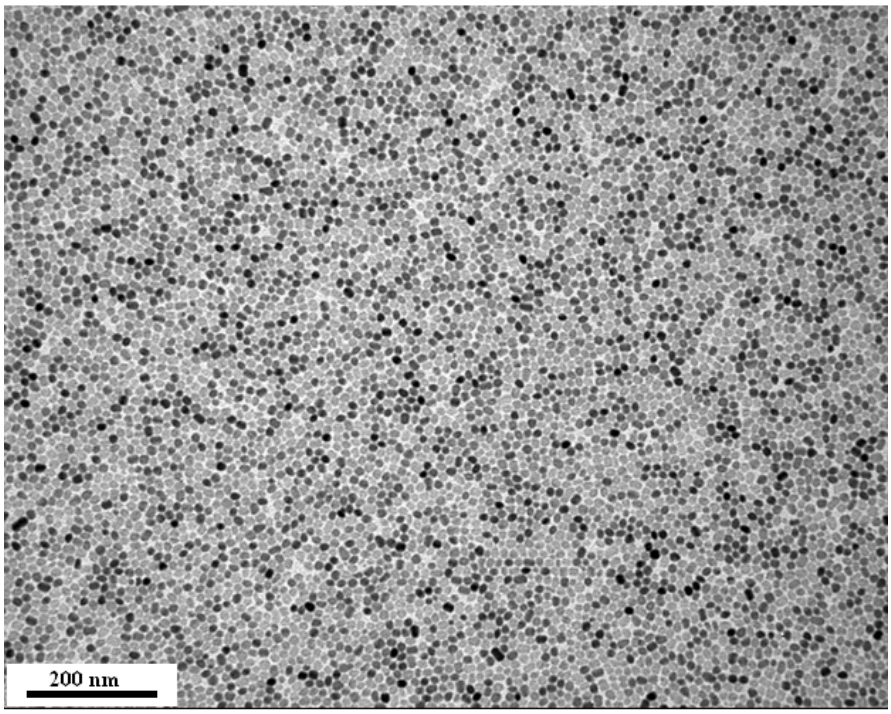

Figure S1. Low magnification TEM image of truncated rhombic shape TiO_2 obtained at TB:OA:OM = 1:5:5.

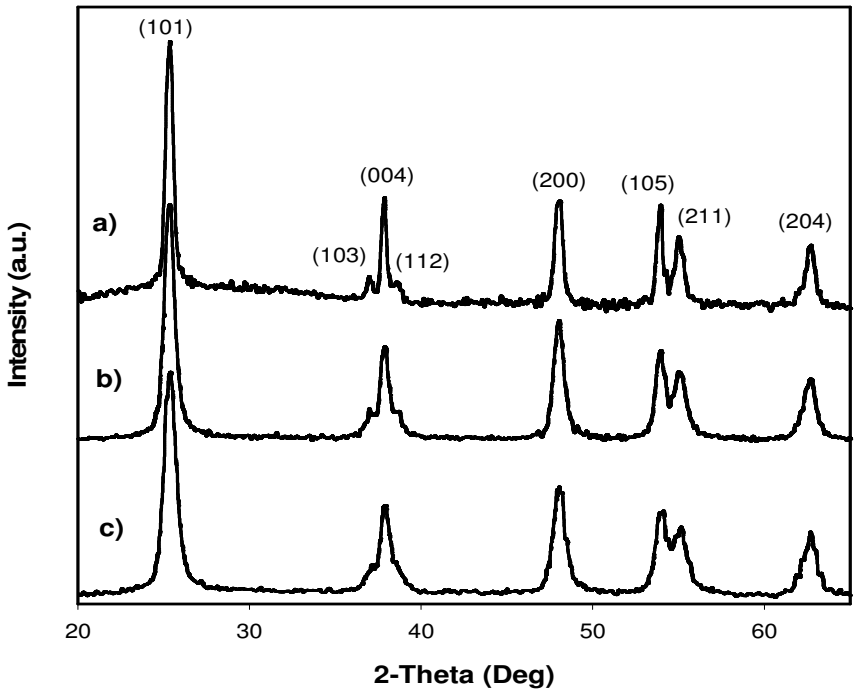

Figure S2. XRD patterns (a) rhombic shape obtained at TB:OA:OM = 1:4:6; (b) truncated rhombic shape obtained at TB:OA:OM = 1:5:5; (c) spherical shape obtained at TB:OA:OM = 1:6:4.

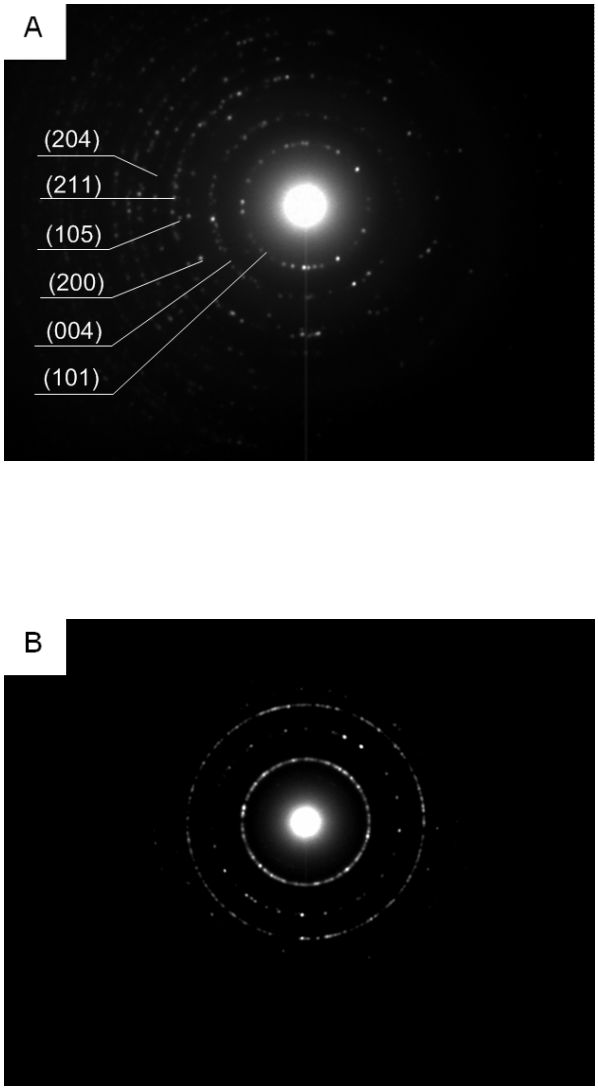

Figure S3. SAED images of (A) rhombic shaped TiO_2 and (B) spherical shaped TiO_2.

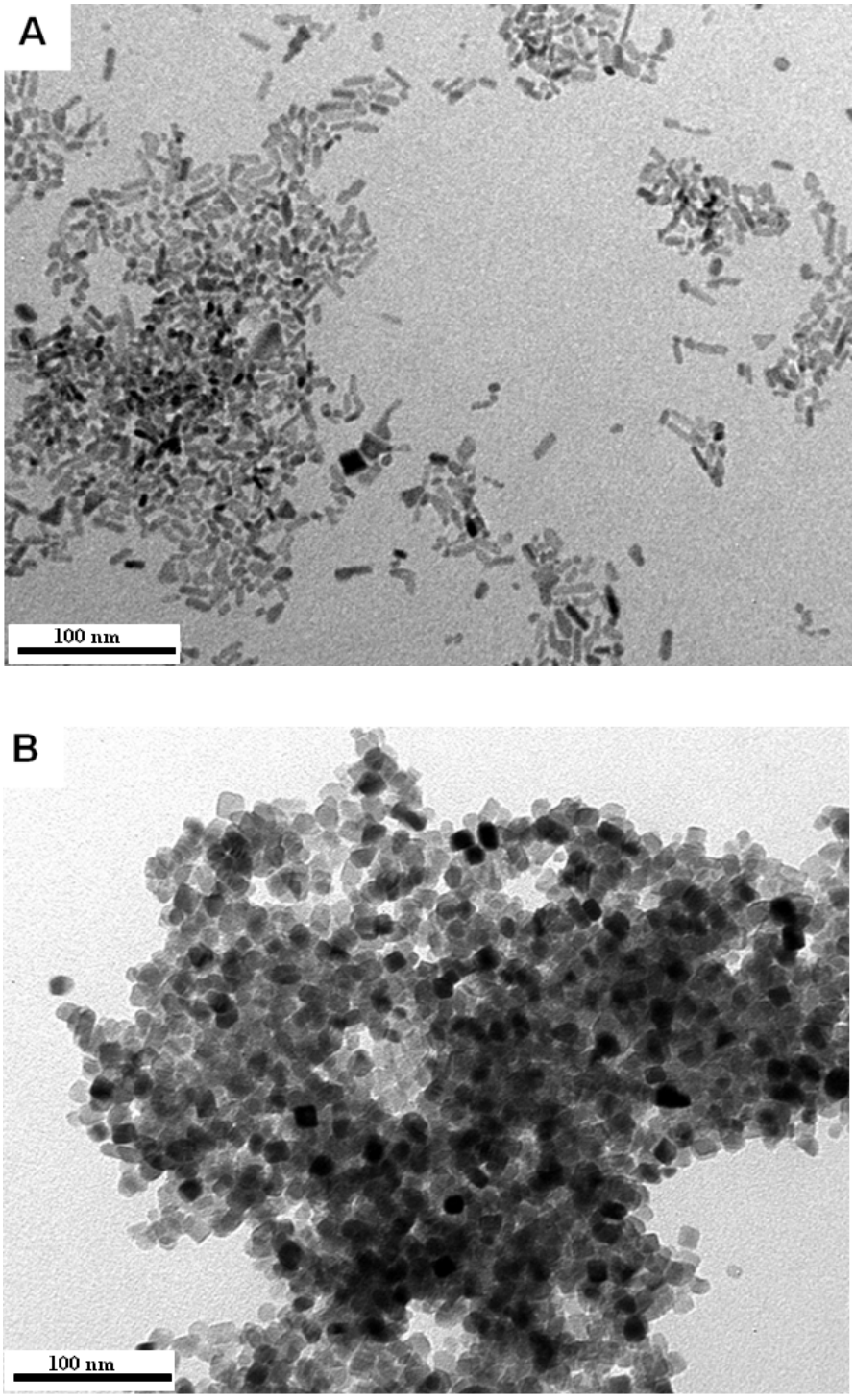

Figure S4. TEM images of TiO_2 nanocrystals obtained (A) with pure ethanol vapor; (B) with pure water vapor (TB:OA:OM = 1:6:4).

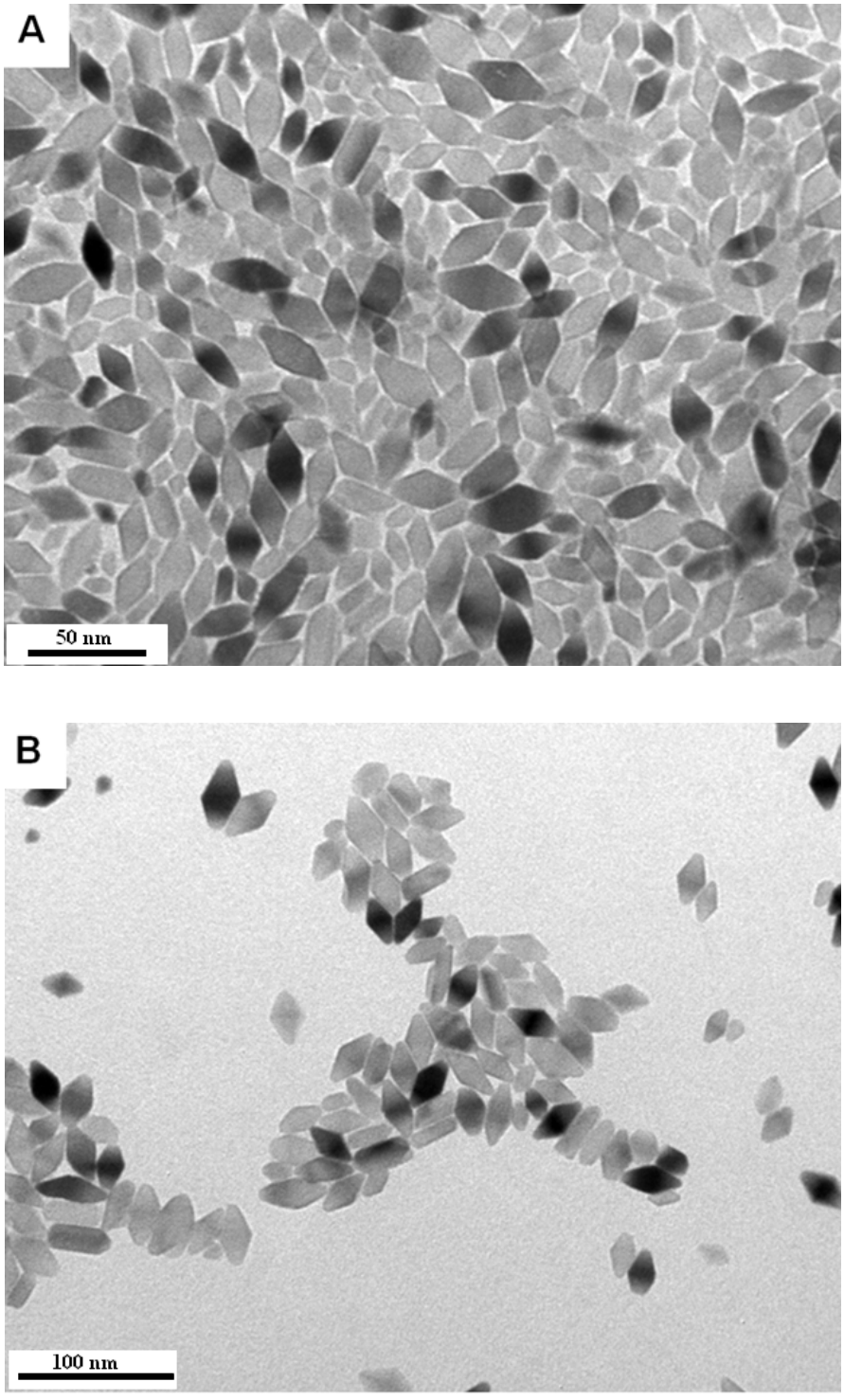

Figure S5. TEM images of rhombic shaped TiO_2 obtained at low OA:OM ratios: (A) TB:OA:OM = 1:2:8, and (B) TB:OA:OM = 1:3:7.

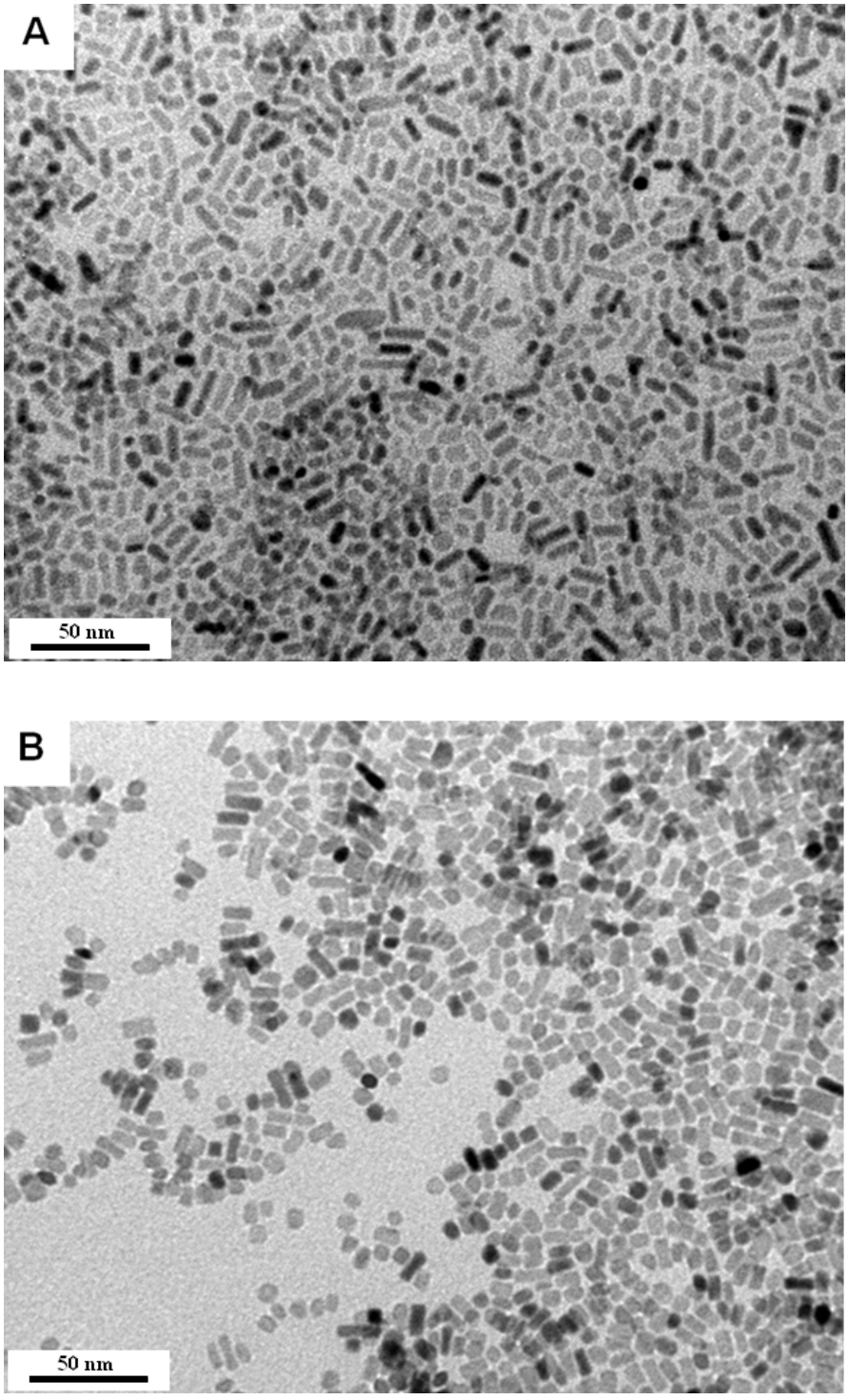

Figure S6. TEM images of nanodot TiO_2 obtained at high OA:OM ratio: (A) TB:OA:OM = 1:8:2, and (B) TB:OA:OM = 1:7:3.

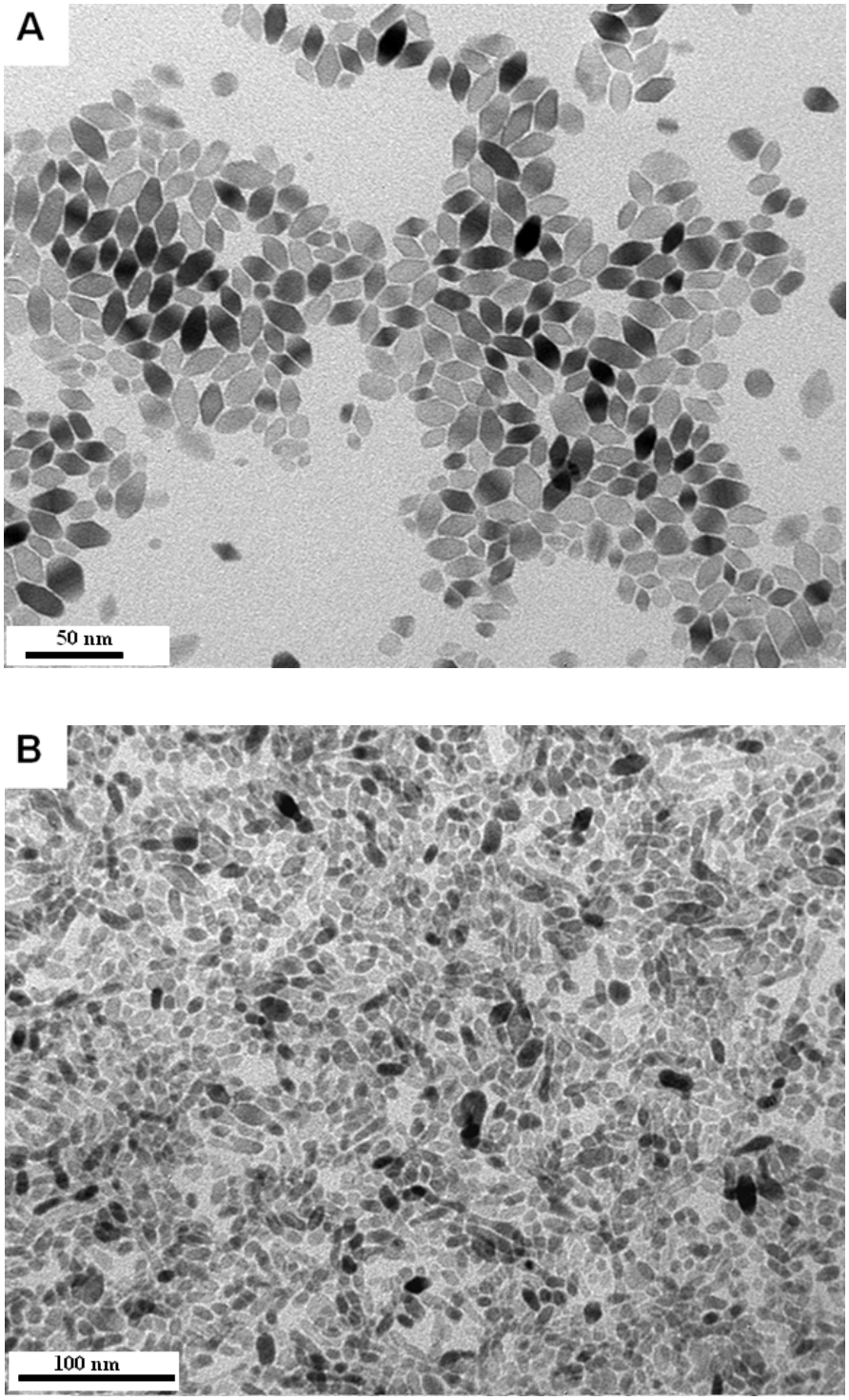

Figure S7. TEM images of TiO_2 nanocrystals obtained using only one surfactant: (A) with OM, TB:OM = 1:5, and (B) with OA, TB:OA = 1:5.

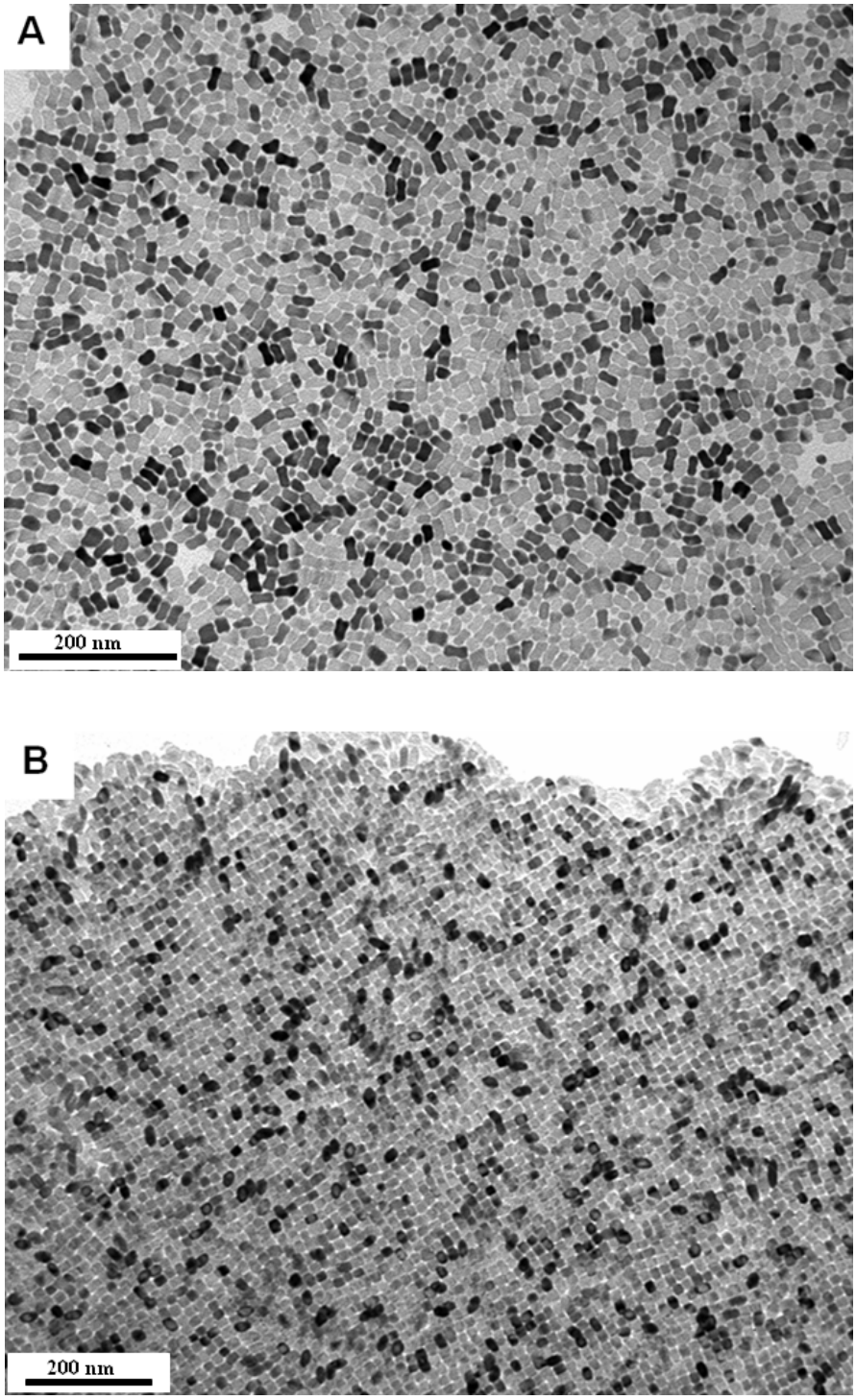

Figure S8. Low magnification TEM images of (A) dog-bone shaped TiO_2 obtained with TB:OA:OM = 2:6:4, and (B) truncated and elongated rhombic TiO_2 obtained with TB:OA:OM = 2:5:5.

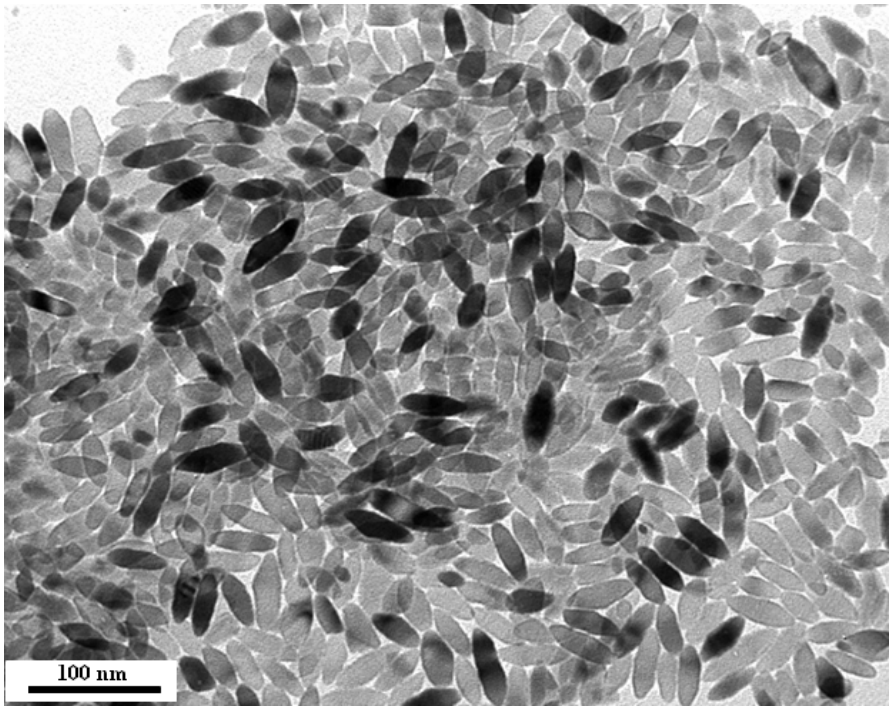

Figure S9. TEM image of elongated rhombic TiO_2 obtained with TB:OA:OM = 2:4:6.

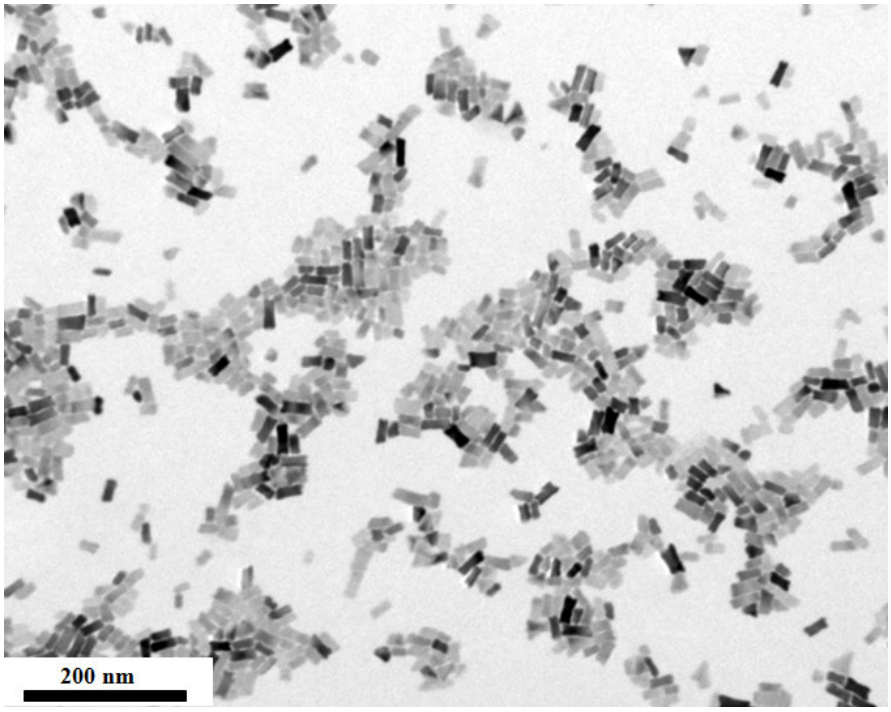

Figure S10. TEM image of TiO_2 nanocrystals obtained with TB:OA:OM = 4:6:4.

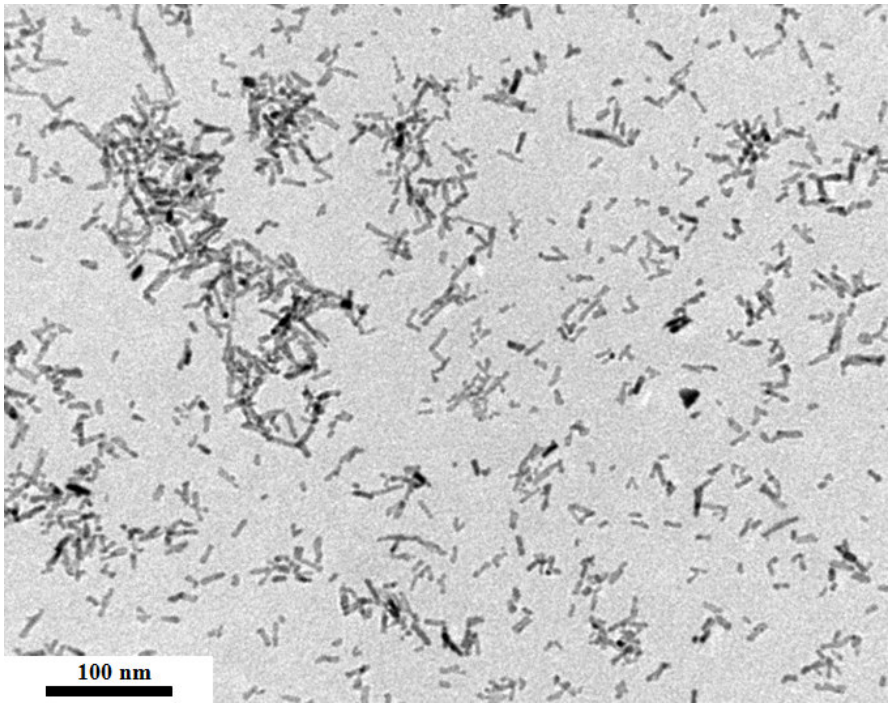

Figure S11. TEM image of TiO_2 nanocrystals obtained with TB:OA:OM = 1:6:4 at 120 ^{o}C.

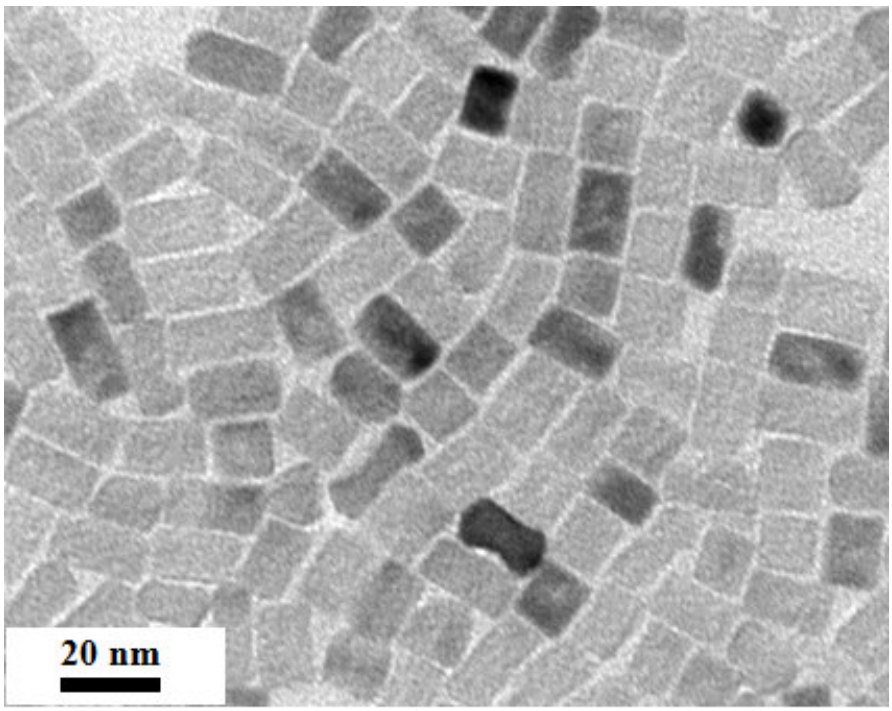

Figure S12. High-magnification TEM image of TiO_2 nanocrystals obtained with TB:OA:OM = 1:6:4 at 140 ^{o}C.

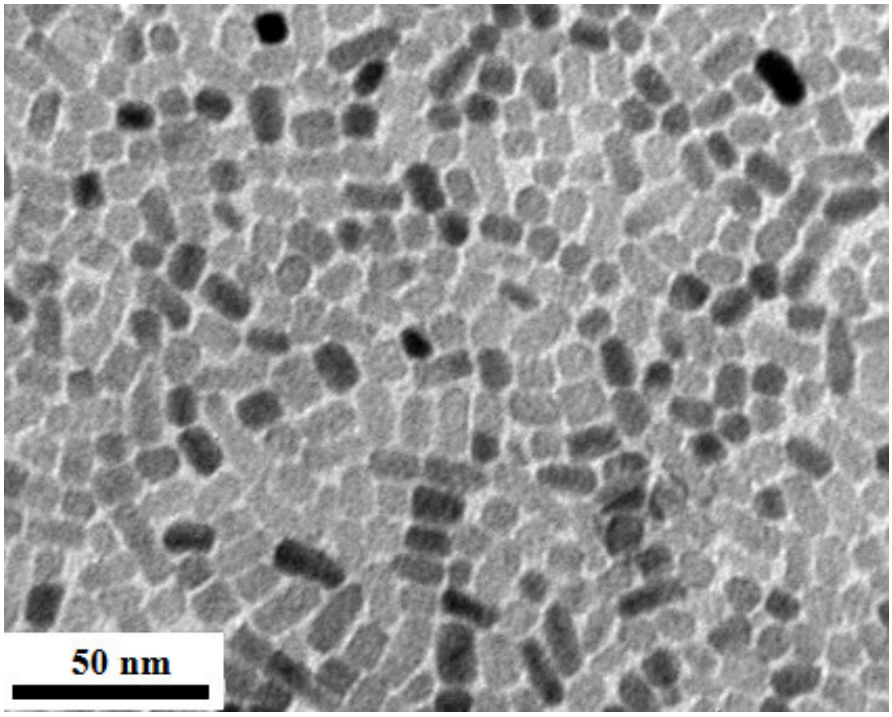

Figure S13. TEM image of TiO_2 nanocrystals obtained with TB:OA:OM = 1:6:4 at 160 ^{o}C.

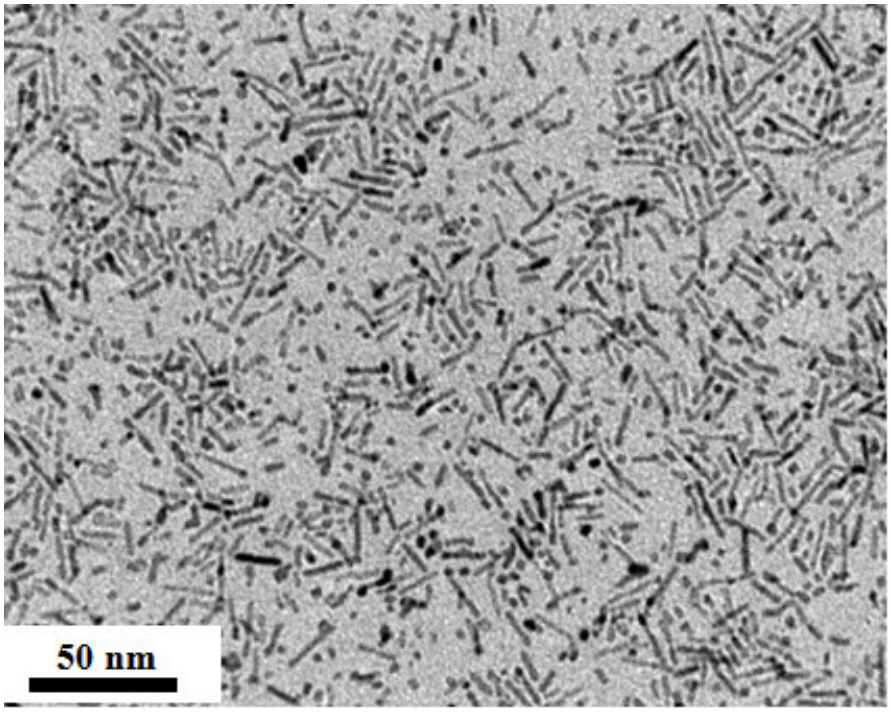

Figure S14. TEM image of TiO_2 nanocrystals obtained with TB:OA:OM = 1:8:2 at 140^{o}C